Absorption Spectra and Geometries of Ar N + (N) 30-60)

ARTICLE · JULY 2001

DOI: 10.1021/jp0100102

2 AUTHORS:

José A Gascón
University of Connecticut
60 PUBLICATIONS **1,420** CITATIONS
SEE PROFILE

Randall W. Hall
Dominican University of California
57 PUBLICATIONS **876** CITATIONS
SEE PROFILE

Absorption Spectra and Geometries of Ar_N^+ ($N = 30-60$)†

José A. Gascón‡ and Randall W. Hall*,§

Departments of Chemistry and Physics and Astronomy, Louisiana State University, Baton Rouge, Louisiana 70803

Received: January 3, 2001; In Final Form: March 23, 2001

We report finite temperature simulations of Ar_N^+ ($N = 30-60$) using a semiempirical model Hamiltonian. We calculate the photoabsorption spectra and analyze the charge distribution in both ground and excited states. The maximum photoabsorption wavelength for this set of clusters is in good agreement with experimental data. We analyze the average position of the atoms and the finite temperature distribution of the positive charge over the cluster. We find the charge localized on three atoms in the ground state and over the first two solvation spheres in the excited states. The extent of delocalization in the excited states can be correlated with the shift in the maximum photoabsorption wavelength.

1. Introduction

One of the primary goals of cluster science is to understand the evolution of physical properties from atoms to nanoparticles and finally to the bulk. The rich variety of processes that have been studied during the last 30 years include ion solvation, electron solvation, coulomb explosions, and surface effects.[1] In the past few years, electronic and structural properties of rare gas cation clusters have received considerable attention. The interplay between experiment and theory has generated a vibrant discussion. These systems allow the investigation of properties related to some of the processes mentioned above, including questions about charge delocalization, polarization effects, and magic numbers. A main point of discussion is whether the charge is localized in a dimer or a trimer core and how the size of the core evolves with cluster size. Experimental results by Levinger et al.[2] and Haberland et al.[3] on the photoabsorption of Ar_N^+ present strong evidence that, in the ground state, the charge is localized in a linear trimer core that persists as the size of the cluster increases. This result was supported theoretically by groups using a simple model,[4] diatomics-in-molecules (DIM) calculations,[5−10] and ab initio constructed potential energy surfaces[11−13] and by our group using a semiempirical model.[14,15] Another DIM model found a linear tetramer core[16] for some of the larger clusters. The origin of the delocalization is a result of the overlap of p-orbitals due to the hole created upon ionization. Another effect is the increased stability of the cluster compared to its neutral species as a result of the polarization of the neutral atoms by the charged core. This last effect has motivated the inclusion of many-body polarization in the theoretical models[6,15−18] that can be important in highly polarizable clusters such as Ar and Xe. In a previous study,[15] we included many-body polarization and found good agreement between our results and experimental results for clusters of size $N = 2-27$. We found, as have others,[8] that the charge is localized on three atoms in the electronic ground state and is delocalized over a significant number of other atoms in the excited states. This delocalization in the excited states occurred using models with and without many-body polarization. Further, we found that inclusion of many-body polarization was most important primarily for smaller clusters ($N < 10$) and that the difference between our model with and without polarization became small for clusters sizes greater than about 20 atoms. In this work, we extend our simulations to $N = 60$ to probe two important issues: whether the charge remains localized on three atoms for these larger clusters in the ground state and whether the delocalization of charge over the entire cluster continues as atoms are added to the cluster in the excited states. We use our model without many-body polarization in these studies to minimize computational effort and because we found only small differences between the two models for larger cluster sizes.

2. Monte Carlo Procedure, Results, and Discussion

The model Hamiltonian used here is described in our previous work[15] and will not be detailed here. We used the version of the Hamiltonian without many-body polarization. We performed Monte Carlo calculations at 80 K, using the following procedure: the initial configuration was generated by using a genetic algorithm to find the lowest energy geometry of a neutral *N*-atom cluster subject to a Lennard−Jones potential. From this initial configuration, a Monte Carlo simulation of 20 000 steps was performed at a temperature of 80 K. At each step, the $3N \times 3N$ Hamiltonian was diagonalized to find the ground and excited states. We used the ground-state geometry in the Monte Carlo sampling process and used the excited states to calculate the average photoabsorption spectra as described in ref 15 for cluster sizes in the range $N = 30-55$. Because of the large computational effort, we did not calculate the photoabsorption spectrum for $N = 60$; however, we still sampled 20 000 configurations using an approximation that will be describe below (see the comments in Figure 1). These configurations were used in the charge distribution analysis.

We also attempted to calculate the lowest-energy geometries for some clusters that were reported to be the most stable clusters in an experiment performed by Harris et al.[19] They found magic numbers at $N = 32$, 34, 43, 46, 49, and 55 in the range $N = 30-60$. Global optimization of these medium size clusters presented a formidable task. However, at this point, it was

† Part of the special issue "Bruce Berne Festschrift".

* Corresponding author. Phone: (225)578-3472. Fax: (225)578-3458. E-mail: rhall@lsu.edu.

‡ Department of Chemistry. E-mail: jgascon@lsu.edu.

§ Departments of Chemistry and Physics and Astronomy.

10.1021/jp0100102 CCC: $20.00
Published on Web 05/09/2001

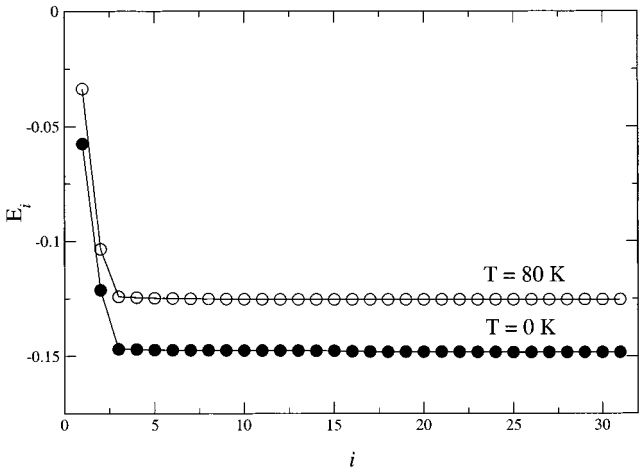

Figure 1. Ground-state energy as a function of the effective number of atoms that determine the dimension of the matrix Hamiltonian.

already known that the charge is localized mainly in a trimer core. This suggested that we consider an effective number of atoms on which the charge could have significant amplitude. Similar approximations have been proposed before.[4,19] Within our model Hamiltonian, this is equivalent to making the size of the matrix as small as 9×9 (the charge can be in any of the 3-p orbitals on each of the three core atoms). Figure 1 shows that such approximation is very reasonable. It displays, for $N = 31$, the ground-state energy as a function of the number of atoms allowed to have charge. Here, atoms are sorted in order of decreasing charge in the ground state. Therefore, in our search for the lowest-energy structures, we made the approximation that the charge was localized on a three-atom core. From the Monte Carlo sampling described above, we saved configurations every 200 steps. The 1000 saved configurations for each cluster size were then minimized using a conjugate gradient algorithm, subject to our approximation. The value of 0 K indicates that the energy was calculated using the lowest-energy geometry found in our conjugate gradient minimizations, while 80 K indicates that the energy was calculated as an average from the Monte Carlo sampling. In any case, it is clear that confining the charge to be on the first three atoms gives a good approximation to the total energy. Therefore, we used such approximation in the conjugate gradient method to search for the global energy for the cluster sizes mentioned above. Some of these geometries are shown in Figure 2. There is a noticeable cylindrical symmetry for these clusters, reflecting the cylindrical symmetry of the three-atom charged core. A common structure for the clusters in this range is a 25-atom core formed by five atoms (the middle three of which are the three-atom core) relatively in line and four rings of five atoms each between two adjacent atoms. In fact, this is the lowest-energy geometry of the 25 atom cluster.[6,8]

Our results for the photoabsorption spectra are shown in Figure 3, along with a comparison to the work of Haberland et al.[3] The position of the maximum peak was obtained by fitting a Gaussian function to the main peak. Figure 4 shows the spectrum for $N = 50$ along with the Gaussian. As can be seen, there is good agreement between theory and experiment for the location of the maximum in the photoabsorption spectrum. However, according to our data, there is still a small red shift. As we will see later, this may be due to a small, but continued, delocalization of the positive charge over the cluster for those excited states that contribute to the main photoabsorption peak.

We now turn to the charge distribution in both the ground and excited states. The average is done using the 1000 saved configurations from the Monte Carlo sampling. In performing the average, the square of the transition dipole is used as a weighting factor. Shown in Figure 5 are our results for the charge distribution in the ground state as a function of the *i*th atom ($1 \leqslant i \leqslant N$). Here, atoms are enumerated in order of decreasing charge in the ground state. Two representative clusters of the whole range are displayed, $N = 30$ and $N = 55$. There appears to be no change in the three-atom core seen in smaller clusters. The asymmetry seen between the second and third atom is due to our numbering scheme and reflects the instananeous difference in the two bond lengths resulting from the asymmetric normal mode vibration. Figure 6 shows the charge distribution for those excited states contributing to the main peak for $N = 35$, 50, 55, and 60. The figure at the bottom is an augmented view of the upper figure. It can be seen that the charge continues to delocalize over the entire cluster, even between $N = 50$ and $N = 55$. However, the results from $N = 60$ are in very close agreement with $N = 55$, suggesting that the delocalization has ended at $N = 55$, corresponding to the completion of the second solvation shell. This may explain the small red shift in the photoabsorption peak we find between $N = 43$ and $N = 55$. We further analyzed the charge distribution of the excited states by calculating both the radial distribution

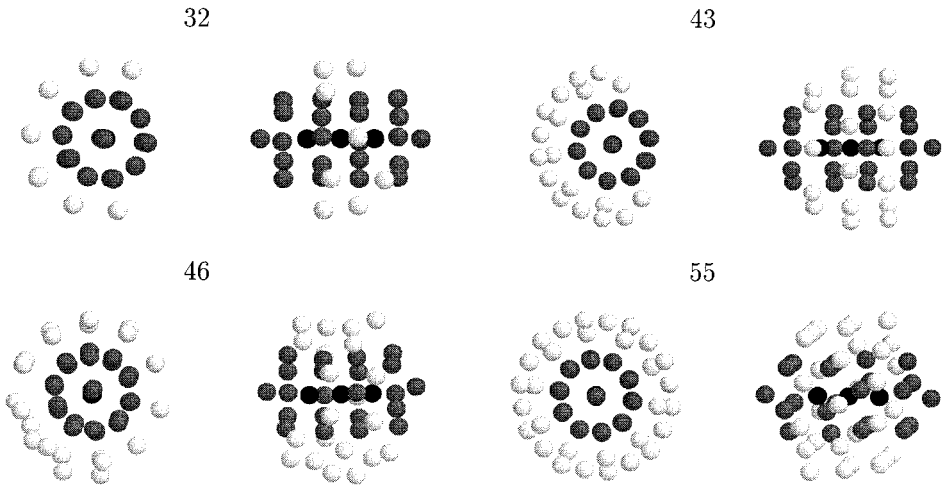

Figure 2. Lowest-energy geometries for some representative clusters. For each cluster, a front view and a side view are displayed. The radii of the atoms are reduced for clarity. The three atoms that carry the charge in the ground state are colored black, the next 22 atoms that complete the first solvation shell are colored gray, and the atoms forming the second solvation shell are colored white.

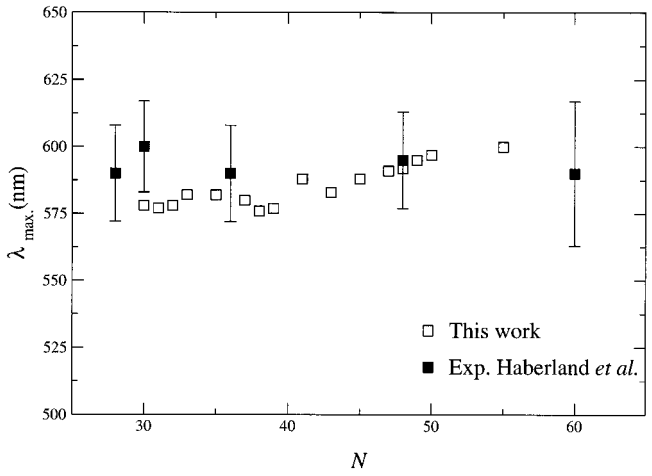

Figure 3. Experimental and computed photoabsorption maxima, as a function of cluster size. The experimental work is from ref 3, and the computed maxima were obtained with a Gaussian fit to the peak.

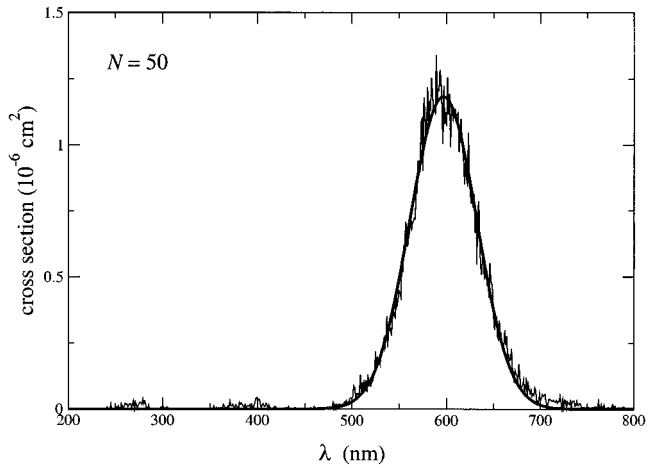

Figure 4. Calculated and fit to $N = 50$ photoabsorption spectrum. The solid line is the result of a Gaussian fit done to estimate the maximum wavelength.

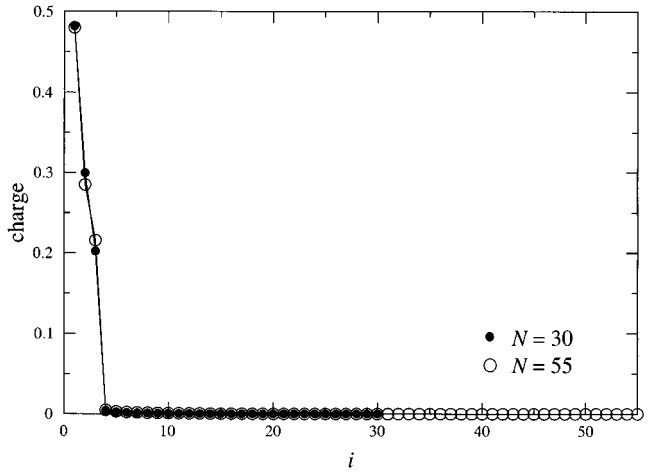

Figure 5. Charge distribution in the ground state, as a function of atom number. Atoms were numbered in decreasing order of charge.

of the charge and the radial distribution of the atomic positions. This was done by locating atom 1 on the origin and atom 2 on the *z*-axis. Thus, all distances were measured to the *z*-axis. Our results are shown in Figure 7 for selected clusters. The dark line on these figures corresponds to the radial distribution of the atomic positions, while the light line corresponds to the radial charge distribution. The sharp peak at $\rho = 0$ of the atomic

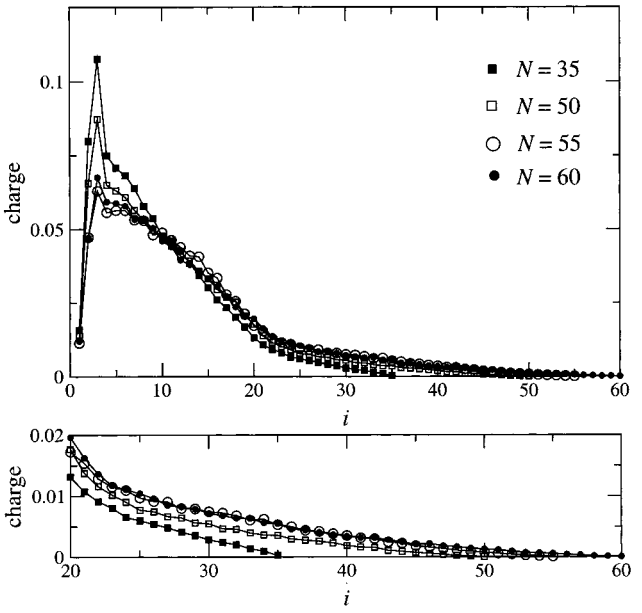

Figure 6. Charge distribution for the excited states, as a function of atom number. Atoms were numbered in decreasing order of charge in the ground state. The figure at the bottom is an augmented view of the upper figure.

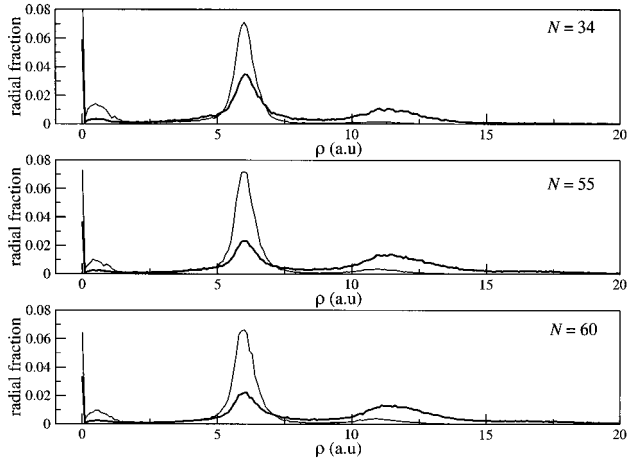

Figure 7. Charge distribution for the excited states (light line) and atomic distribution (dark line), as a function of the radial distance to the *z*-axiz. The *z*-axiz is defined to contain atom 1 and 2.

positions distribution corresponds, by definition, to atoms 1 and 2. The small peak at $\rho \simeq 0.5$ au contains the contribution from two atoms, atoms that are almost aligned with the *z*-axis (one of which is most likely the third atom in the three-atom core). The peak at $\rho \simeq 6$ au corresponds to the first solvation shell. Integration of this peak indicates there are approximately 20 atoms in this shell. In particular, it contains 18 atoms for N = 34, 21 atoms for $N = 55$, and 23 atoms for $N = 60$. Integration of the charge distribution indicates that roughly 90% of the charge is confined to these atoms, adding roughly to 25 atoms (core + first solvation shell). The third peak corresponds to the second solvent shell. It contains 11, 23, and 25 atoms for $N =$ 34, 55, and 60, respectively. At 0 K, one would not expect to find atoms outside the second shell for $N \leqslant 55$. However, at finite temperatures, there will be some atoms in the third shell (which we defined to be around $\rho \simeq 16$ au). Integration of this peak contributes 1, 7, and 8 atoms for $N = 34$, 55, and 60, respectively. Thus, although there are some atoms in the third shell, it can be seen that there is practically no charge on those atoms. Therefore, we find that the excited-state charge delo-

calizes over the core, first, and second solvent shell supporting the tendency of the shift of the maximum wavelength to reach its bulk value beyond $N \leqslant 55$.

3. Conclusions

We have used our semiempirical model to study larger argon cation clusters. We find good agreement between our results and the experimental work of Haberland[3] for the position of the photoabsorption peak. Analysis of the ground electronic state demonstrates that the charge is localized in a three-atom core for all cluster sizes studied. The excited states that contribute to the photoabsorption peak demonstrate charge delocalization over many atoms, up to the second solvation shell. Our calculation for $N = 60$ indicates no further charge delocalization for the excited state when a third solvation shell is added. The geometries found for these clusters are of cylindrical symmetry, corresponding to the linear, three-atom charged core in the ground state.

Our calculations suggest that the excited states correspond to charge delocalization of the first and second solvation shells. The cluster sizes studied here are about half the size of the smallest stable doubly charged Ar clusters, where stable Ar_N^{2+} clusters occurs at around $N = 90$,[20−22] or about twice the number of atoms need to "contain" the excited state charge in a singly charged cluster. As our model can be modified to treat doubly charged clusters, such a study will be the focus of future work.

References and Notes

(1) Castleman, A. W.; Bowen, K. H. *J. Phys. Chem.* **1996**, *100*, 12911.

(2) Levinger N. E.; Ray, D.; Alexander, M. L.; Lineberger, W. C. *J. Chem. Phys.* **1988**, *89*, 5654.

(3) Haberland, H.; Issendorff, B. V.; Kornmeier, H.; Orlik, W.; Kolar, T.; Ludewigt, C.; Reiners, T.; Risch, A. In *Physics and Chemistry of Finite Systems: From Clusters to Crystals*; Ed. Jena, P.; Kluwer; Dordrecht, The Netherlands, 1992; Vol. II.

(4) Gianturco, F. A.; Buonomo, E.; Delgado-Barrio, G.; Miret-Artés, S.; Villarreal, P. *Z. Phys. D* **1995**, *35*, 115.

(5) Last, I.; George, T. F. *J. Chem. Phys.* **1990**, *93*, 8926.

(6) Doltsinis, N. L.; Knowles, P. J.; Naumkin, F. Y. *Mol. Phys.* **1999**, *96*, 749.

(7) Ikegami, T.; Iwata, S. *J. Chem. Phys.* **1996**, *105*, 10734.

(8) Ikegami, T.; Kondow, T.; Iwata, S. *J. Chem. Phys.* **1993**, *98*, 3038.

(9) Kuntz, P. J.; Valldorf, J. *Z. Phys. D* **1988**, *8*, 195.

(10) Ikegami, T.; Iwata, S. *J. Chem. Phys.* **1999**, *110*, 8492.

(11) Kirkwood, D. A.; Woodward, C. A.; Mouhandes, A.; Stace, A. J.; Bastida, A.; Zuniga, J.; Requena, A.; Gadéa, F. X. *J. Chem. Phys.* **2000**, *113*, 2175.

(12) Gadéa, F. X.; Savrda, J.; Paidarova, I. *Chem. Phys. Lett.* **1994**, *223*, 369.

(13) Buonomo, E.; de Lara-Castells, M. P.; Gianturco, F. A. *Z. Phys. D* **1997**, *41*, 211.

(14) Morales, G. A.; Faulkner, J.; Hall, R. W. *J. Chem. Phys.* **1998**, *109*, 3418.

(15) Gascon, J. A.; Hall, R. W. *J. Chem. Phys.* **2000**, *113*, 7204.

(16) Doltsinis, N. L.; Knowles, P. J. *Mol. Phys.* **1998**, *94*, 981.

(17) Cao, J.; Berne, B. J. *J. Chem. Phys.* **1992**, *97*, 8628.

(18) Grigorov, M.; Spiegelmann, F. *Surf. Rev. Lett.* **1996**, *3*, 211.

(19) Harris, I. A.; Kidwell, R. S.; Northby, J. A. *Phys. Rev. Lett.* **1984**, *53*, 2390.

(20) Scheier, P.; Märk, T. D. *J. Chem. Phys.* **1987**, *86*, 3056.

(21) Stace, A. J.; Lethbridge, P. G.; Upham, J. E. *J. Chem. Phys.* **1989**, *93*, 333.

(22) Gotts, N. G.; Lethbridge, P. G.; Stace, A. J. *J. Chem. Phys.* **1992**, *96*, 408.